

## CFD Analysis of NACA 2421 Aerofoil at Several Angles of Attack

Varatharajan R Madhanraj\* and Dilip A Shah

Department of Aeronautical Engineering, Hindustan Institute of Technology and Science, Chennai, Tamil Nadu, India

### ABSTRACT

In this paper NACA 2421 Aerofoil is analyzed at several angles of attack ranging from -200 to 200 and with the Reynolds number at  $1.8 \times 10^5$  and the velocity are 20 m/s. The co-efficient of lift and drag are compared with the standard values in the literature. Variation of pressure co-efficient is plotted in the form of contour. The aerofoil is designed in ANSYS and it is imported to Computational Fluid Dynamics and the variations of CL and CD with respect to various angles of attack is analyzed.

**Keywords:** Computational fluid dynamics; Aerofoil; Angle of attack; Stalling

### INTRODUCTION

The NACA 2421 Aerofoil is designed for subsonic aircraft wings because of the better performance. Significance of improving a UAV performance can be done at very low Reynolds number  $1.8 \times 10^5$ . Flow separation occurs normally due to very low inertia and very high viscosity [1]. In general NACA 2421 Aerofoil generates more lift in subsonic speed.

### OBJECTIVE

As per the Bernoulli's principle if the pressure increases the velocity will decrease and vice versa [2]. Due to this pressure difference the lift is generated. In this work the flow separation over NACA 2421 unsymmetrical airfoil is observed and steps are taken to increase the lift to drag ratio [2].

### PROBLEM DEFINITION

In this work the stalling region is analyzed, and the various angles of attack is also analyzed [3]. For all type of NACA series the lift to drag ratio is very important criteria for the Aircraft design. Here the lift to drag ratio, critical angles of attack and stall regions are analyzed over the NACA 2421 Aerofoil with the various angles of attack [1].

### MATERIALS AND METHODS

#### SST turbulence model

Shear Stress Transport ( $k-\omega$ ) is used as a low turbulence model. It will often the good behaviour in adverse pressure gradients and separating the flow [3]. It is used to predict the effect of turbulence.

(i) Turbulence Kinetic Energy:

$$\frac{\partial k}{\partial t} + U_j \frac{\partial k}{\partial x_j} = P_k - \beta^* k \omega + \frac{\partial}{\partial x_j} \left[ (v + \sigma_K v_T) \frac{\partial k}{\partial x_j} \right]$$

(ii) Specific Dissipation Rate:

$$\frac{\partial \omega}{\partial t} + U_j \frac{\partial \omega}{\partial x_j} = \alpha S^2 - \beta \omega^2 + \frac{\partial}{\partial x_j} \left[ (v + \sigma_K v_T) \frac{\partial \omega}{\partial x_j} \right] + 2(1 - F_1) \sigma_{\omega} \frac{1}{2\omega} \frac{\partial k}{\partial x_i} \frac{\partial \omega}{\partial x_i}$$

F1-Blending Function

$$F_1 = \tanh \left\{ \min \left[ \max \left( \frac{\sqrt{k}}{\beta^* \omega y}, \frac{500v}{y^2 \omega} \right), \frac{4\sigma \omega^2 k}{CD_{K\omega} y^2} \right] \right\}^4 \quad F1=1 \quad \text{inside}$$

the Boundary Layer

F1=0 in the free stream

CDK  $\omega$

\*Correspondence to: Varatharajan Raj Madhanraj, Department of Aeronautical Engineering, Hindustan Institute of Technology and Science, Chennai, Tamil Nadu, India, Tel: +919488683240; E-mail: mtechmadhan@gmail.com

Received: January 02, 2019; Accepted: May 31, 2019; Published: June 04, 2019

Citation: Madhanraj VR, Shah DA (2019) CFD Analysis of NACA 2421 Aerofoil at Several Angles of Attack. J Aeronaut Aerospace Eng 8: 216. doi: 10.35248/2168-9792.19.8.217

Copyright: © 2019 Madhanraj VR, et al. This is an open-access article distributed under the terms of the Creative Commons Attribution License, which permits unrestricted use, distribution, and reproduction in any medium, provided the original author and source are credited.

$$CD_{K\omega} = \max\left(2\rho\sigma\omega^2 \frac{1}{\omega} \frac{\partial k}{\partial x_i} \frac{\partial \omega}{\partial x_i}, 10^{-10}\right)$$

Kinematic Eddy Viscosity

$$\nu_T = \frac{a_1 k}{\max(a_1 \omega, SF_2)}$$

F2 - Second Blending Function

$$F_2 = \tanh\left\{\left[\min\left[\max\left(\frac{2\sqrt{K}}{\beta^* \omega y}, \frac{500\nu}{y^2 \omega}\right)\right]\right]^2\right\}$$

Pk- Production Limiter

$$P_K = \min\left(\tau_{ij} \frac{\partial U_i}{\partial x_j}, 10\beta^* k\omega\right)$$

- The SST model exhibit less sensitivity to free stream conditions,
- The Shear Stress limiter helps the
- $k-\omega$  model to avoid a build-up of excessive turbulence kinetic energy near o the stagnation points,
- The SST model provides the platform for additional extensions such as SAS and laminar to turbulence transition.

### CFD MODELLING AND MESHING

By using the geometry Modeller of Ansys Fluid Flow CFX, the imported co-ordinates are processed to prepare the model. Mesh generation is done by the polygonal mesh [3].

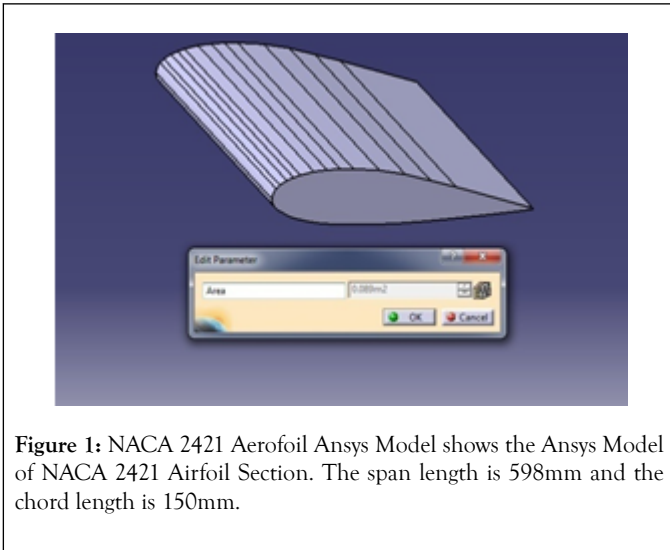


Figure 1: NACA 2421 Aerofoil Ansys Model shows the Ansys Model of NACA 2421 Airfoil Section. The span length is 598mm and the chord length is 150mm.

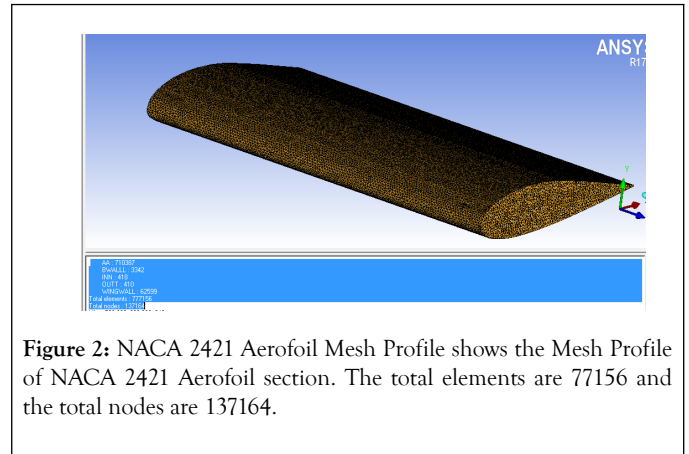


Figure 2: NACA 2421 Aerofoil Mesh Profile shows the Mesh Profile of NACA 2421 Aerofoil section. The total elements are 77156 and the total nodes are 137164.

### BOUNDARY CONDITIONS AND INPUTS

The most fundamental part of CFD problem is to mention the boundary conditions [4]. To conduct the simulation, the boundary condition of the problem some important conditions [3] are needs to be considered as given below.

Various Inputs and Values

- Analysis Type - Steady State,
- Fluid Velocity – 20 m/s,
- Fluid Density – 1 Bar,
- Mach Number – 1.8,
- Turbulence Model – SST,
- Fluid Viscosity –  $1.8 \times 10^{-5}$ ,
- Operating Temperature – 28°C.

### RESULT AND DISCUSSION

Pressure plot and velocity vector

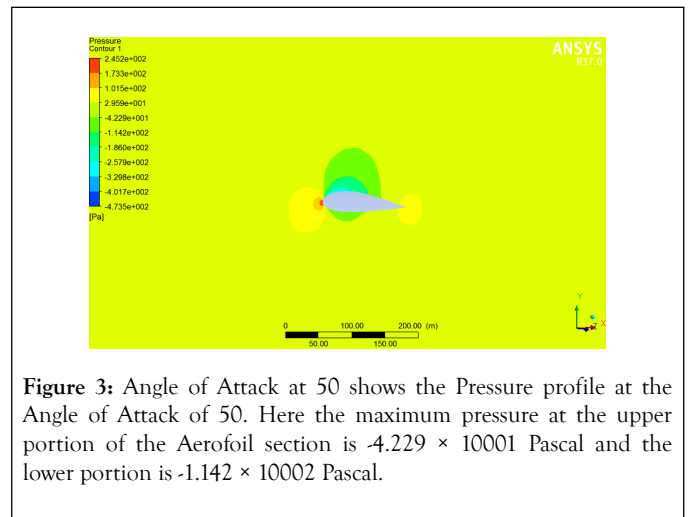


Figure 3: Angle of Attack at 50 shows the Pressure profile at the Angle of Attack of 50. Here the maximum pressure at the upper portion of the Aerofoil section is  $-4.229 \times 10001$  Pascal and the lower portion is  $-1.142 \times 10002$  Pascal.

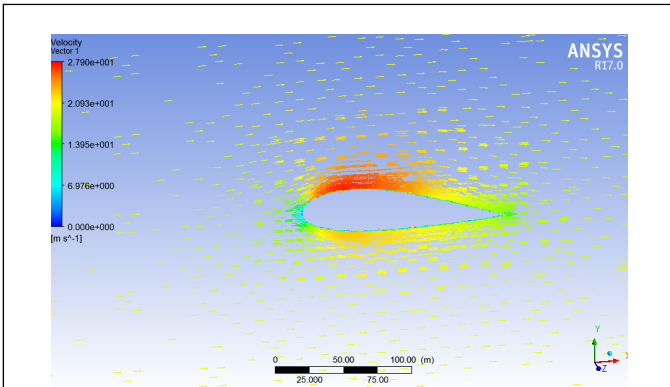


Figure 4: Angle of Attack at 50 shows the velocity profile at the Angle of Attack of 50 and the velocity is 20 m/s.

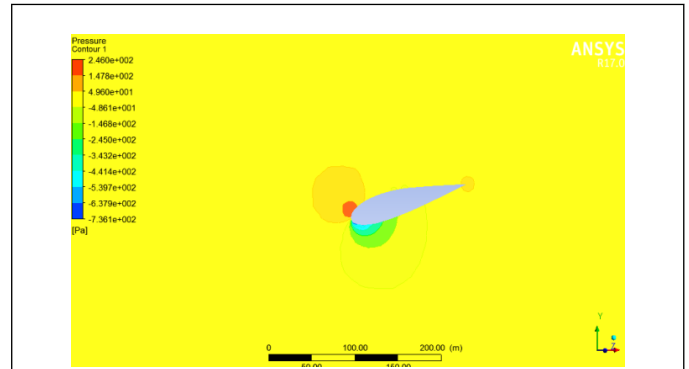


Figure 7: Angle of Attack at -150 shows the Pressure profile at the Angle of Attack of -150. Here the maximum pressure at the upper portion of the Aerofoil section is  $1.47 \times 10002$  Pascal and the lower portion is 0 Pascal. The Angle of Attack at 150 is the stalling angle.

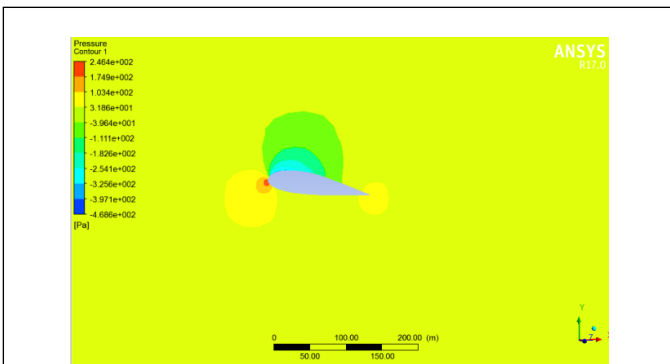


Figure 5: Angle of Attack at 100 shows the Pressure profile at the Angle of Attack of 100. Here the maximum pressure at the upper portion of the Aerofoil section is  $-3.964 \times 10002$  Pascal and the lower portion is 0 Pascal. In the upper portion negative pressure is there. In the lower portion positive pressure is there. This pressure difference tends to the lift generation [5].

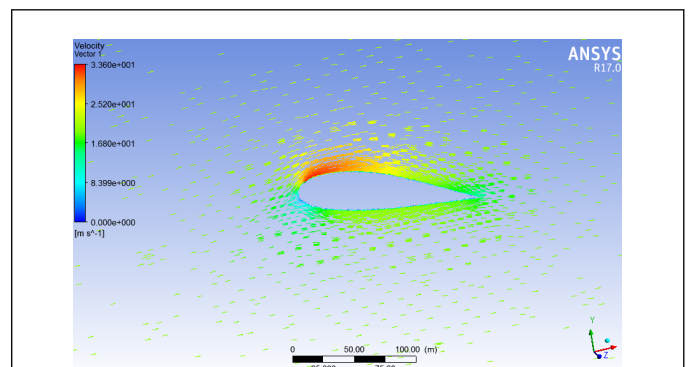


Figure 8: Angle of Attack at 150 shows the velocity profile at the Angle of Attack of 150 and the velocity is 20 m/s From the pressure and velocity plot the co-efficient of lift and the co-efficient of drag values are estimated [1].

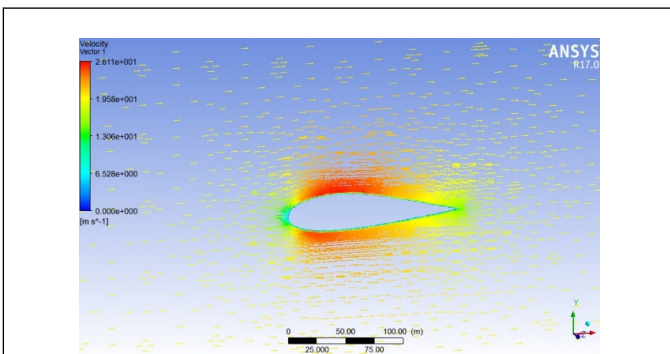


Figure 6: Angle of Attack at 00 shows the velocity profile at the Angle of Attack of 100 and the velocity is 20 m/s.

Table 1: CL and CD Ratios with Various Angles of Attack, the high lift to drag ratio will increases the performance of the aircraft.

$\alpha$	CL CFD	CD CFD
0	0.21	0.008
5	0.67	0.012
10	1.2	0.017
15	1.26	0.029
20	0.8	0.07
-5	-0.32	0.007
-10	-0.83	0.011
-15	-1.1	0.015

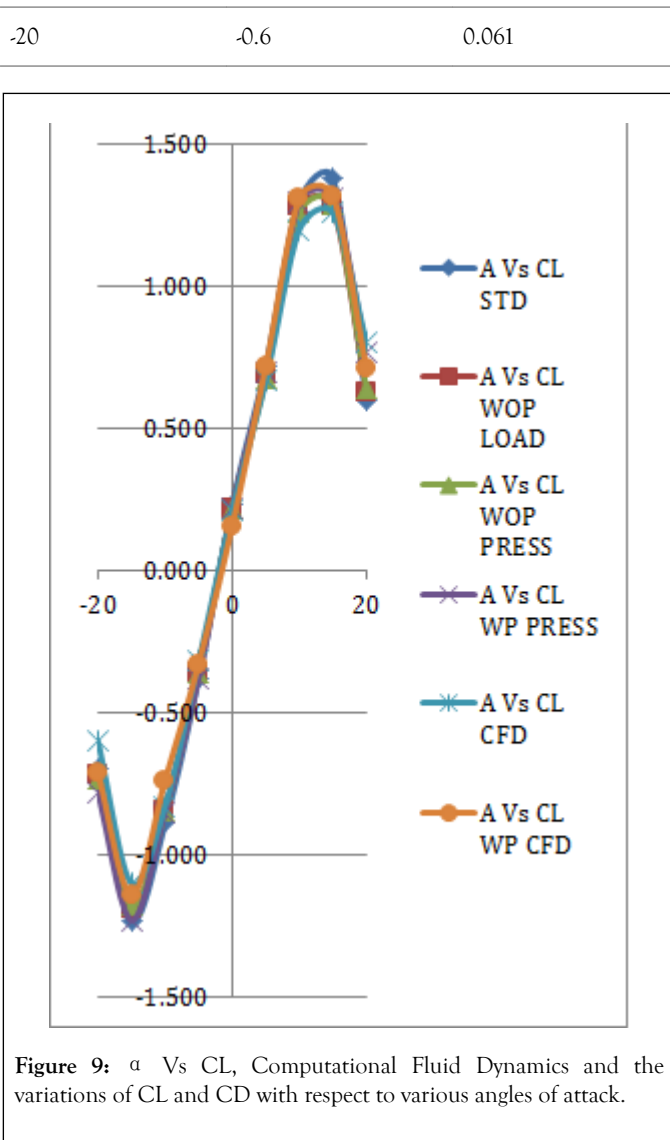


Figure 9:  $\alpha$  Vs CL, Computational Fluid Dynamics and the variations of CL and CD with respect to various angles of attack.

Basically if the angle of attack increases the lift is also increasing up to the certain limit. After the angle of attack reaches  $15^\circ$  the stalling and the critical angle of attack is starting [2]. If the lift is increasing, simultaneously the drag is also increasing (Figures 1-9; Table 1) [1,6].

### CONCLUSIONS

- In all the cases up to the stalling angle if the lift is increases, simultaneously the drag is also increasing.
- The effective angle of attack is  $70$  to  $140$ . Below  $70$  there is very low lift and after  $140$  stalling and the critical angle of attack is reached.
- At the angle of attack is at  $50$  the pressure is  $2.452 \times 10002$  at the top and  $-4.735 \times 10002$  Pascal at the bottom.
- At the angle of attack of  $150$  the pressure is  $2.46 \times 10002$  Pascal at the top and  $-6.159 \times 10002$  Pascal at the bottom.
- The flow separation will affect the generation of lift in the Aerofoil section.

### REFERENCES

1. Zanin P, Pavlenko AM. Control of Flow Separation on a Wing at Low Reynolds Numbers. *J Fluid Dyn* 2012;47(3):403-410.
2. Rumsey CL. Computational Analysis of flow over five different airfoil geometries at high angles of attack. *AIAA J* 2008;87(12): 188.
3. Gad-el-Hak M, Pollard A, Bonnet JP. *Flow Control, Fundamentals and Practices* 1998. Springer Science & Business Media, Germany.
4. Sydney R. Conducted the analysis of the general area of the boundary layer over a smooth surface 1966.
5. Kevadiya M, Vaidya HA. 2D Analysis of NACA 4412 Aerofoil. *Int J Innov Res Sci Eng Technol* 2013;2(5):1686-1691.
6. Sarkar S, Mughal S. CFD Analysis of Effect of Flow over NACA 2412 Airfoil through the Shear stress Transport Turbulence Model. *Int J Mech Pro Eng* 2017;5(7):58-62.